1994

NASA/ASEE SUMMER FACULTY FELLOWSHIP PROGRAM

MARSHALL SPACE FLIGHT CENTER
THE UNIVERSITY OF ALABAMA

THE EFFECT OF FABRICATION ON CORROSION IN ALUMINUM 2195
ENVIRONMENTAL AND MICROSTRUCTURAL CONSIDERATIONS

Prepared by:	Daniel W. Walsh, Ph.D.
Academic Rank:	Professor
Institution and Department:	California Polytechnic State University Department of Materials Engineering
NASA/MSFC:	
Laboratory:	Materials and Processes Laboratory
Division:	Metallic Materials
Branch:	Metallurgy Research
MSFC Colleague:	Merlin D. Danford, Ph.D.

INTRODUCTION

Aluminum alloys containing lithium are particularly attractive to the aerospace structural designer. Lithium's density is only 0.53 g/cc, thus an addition of one weight percent lithium not only increases yield strength, but decreases the density by almost three percent while increasing the modulus by over six percent. The fact that lithium improves these physical properties simultaneously has led to intense study and development of the alloy system. Heretofore, problems in large scale alloy production have retarded comercial development. During the last fifteen years, advances in production technology have rekindled interest in Al - Li alloys, and aluminum suppliers have developed many candidate aerospace materials. However, if these alloys are to be employed successfully, a more complete understanding of their nonequilibrium metallurgy is required. Peel and Starke have each pointed out that an understanding of the weldability of these alloys is a critical step in their implementation. This study addresses the critical lack of information on the environmental compatibility of welded Al 2195 components. Corrosion data for these systems is incomplete, particularly for welded materials exposed to sea water or sea water condensate.

OBJECTIVES

One objective of this investigation was to measure the corrosion rates of welded and as-received Al 2195 samples in 3.5% NaCl and in mild corrosive water (148 mg/l sodium sulfate, 165 mg/l sodium chloride, 138mg/l Sodium carbonate) and to correlate the corrosion rates observed to material microstructure. A parallel set of Al 2219 samples was used to develop a corrosion benchmark. A second objective of this study was to determine the efficiency of organic and inorganic primers for aerospace aluminum alloys.

PROCEDURE

Electrochemical methods were used to determine the corrosion rates in various samples of Alloy2219 and Alloy 2195. These electrochemical measurements were correlated to surface morphology and base/weld metal microstructures as observed by optical microscopy, scanning electron microscopy, electron microprobe analysis and environmental scanning electron microscopy. Al-2219 and Al 2195 samples, welded and unwelded, were exposed to sterile 3.5% NaCl solutions and solutions of mild corrosive water. These samples were monitored using the polarization resistance technique. In addition, Al 2219 samples coated with organic and inorganic primers were exposed to 3.5% NaCl solutions, and studied by AC impedance spectroscopy and polarization resistance techniques. Primer coated samples were also studied as galvanic couples with bare, grit-blasted Al 2219 surfaces.

Measurements of corrosion potential and corrosion rates were made over a period of twenty-five days. Sample discs 1.5 cm in diameter and 0.16 cm thick were used in testing the Al 2195 material as well as the Al 2219 baseline material. These samples were degreased and wiped with alcohol; samples were placed in a holder for exposure to corrosive media. A saturated calomel reference electrode was used in all electrochemical measurements. Primer coated samples were 1/8" X 2" X 5" plates. These samples were exposed in flat cells, both polarization resistance and AC impedance information was collected from these samples.

AC impedance and DC polarization resistance measurements were made on alternate days for the entire test period. AC impedance techniques apply a small amplitude signal of varied frequency to the sample. Electrochemical processes occurring at the surface are modeled as electrical circuits, fourier analysis of the data generated allows the determination of fundamental parameters of the system. The AC impedance data were taken in three sections. The first two sections, beginning at 0.001 Hz and 0.1 Hz, respectively were obtained using the fast fourier transform technique. The last section, ranging from 6.25 to 40,000 Hz was collected using the lock-in amplifier technique. The sequencing was performed automatically using program software, and all data were merged to a single set for each three hour run. After collection the data were processed and analyzed using a personal computer using the model developed by Danford.

Values of the corrosion potential, E_{corr} and the corrosion current, I_{corr} were obtained using the polarization resistance method - the small currents involved disturbed the samples only slightly, and made repeated examination possible. The polarization technique is based on the observation that near E_{corr} the slope of the current - potential graph is nearly constant. The slope is termed the polarization resistance, and is an indicator of the chemical activity in the cell. Stearn and Geary provide an excellent theoretical basis for this technique. One problem with the polarization resistance technique is that it does not indicate whether on not the corrosion is localized. However, in this study, subsequent examination of the sample allowed this to be determined. Polarization resistance data were collected at 0.5 mV intervals at a scan rate of 0.1mV per second. The measurement range for all determinations was -20 to +20 mV with respect to E_{corr} , with all data corrected for IR drop. Data for all polarization resistance scans were analyzed using a commercial program, with a preliminary curve fitting technique as modified by Danford.

RESULTS AND DISCUSSION

Aluminum is a particularly reactive metal - it persists at room temperature because it forms a tenacious oxide film (passivates). An examination of the Pourbaix diagram for aluminum in water indicates that the film is stable in the pH range 4.5 to 8.5 . This stability is limited at actual metal surfaces where the film is attacked by anions in solution, local variations in pH and local changes in oxygen concentration. The presence of second phases, as are found in both Al 2219 and Al 2195 often detract from the stability of passivating films.

Alloy 2219 is basically a binary alloy of aluminum and copper - an age hardening material. Its predecessors, 2014 and 2024 are Al-Cu materials with substantial Mg and Zn added to enhance aging kinetics at low temperatures. Alloy 2219, heat treated in an equivalent fashion is not as strong as 2014 or 2024 at low temperatures, but has superior high temperature strength and weldability. Improved weldability is won by increasing the copper content in the alloy past the limit of solid solubility. Enhanced weldability is promoted by an increased volume fraction of liquid present during critical stages of solidification; cracks form but are backfilled by the plentiful eutectic fluid present. Al 2195 is stronger, lighter and stiffer than Al2219, however it is more difficult to weld, and the character of the weld and HAZ region lead to problems with localized corrosion, particularly with autogenous welds.

Welding is an inherently nonequilibrium process, the severe thermal cycle associated with welding redistributes solutes, engenders transient stress in the weld vicinity, and changes base metal microstructure. The corrosion susceptibility of the Al 2195 alloy can be correlated to the solute redistribution associated with the welding process, and parallels the hot cracking susceptibility of the material in this study. Weld solidification cracking in the aluminum alloys depends upon alloy composition, the solidification temperature range, and the amount and character of the terminal eutectic constituent. At low solute contents, the solidification temperature range is small, and little eutectic forms in the structure. As the solute content increases, the solidification range expands, and the amount of eutectic constituent increases to a level that provides for a thin liquid coating in interdendritic and solidification grain boundaries. Under equilibrium conditions, a maximum cracking propensity is reached at the limit of solid solubility. At compositions in excess of the limit of solid solubility, the solidification range again decreases, and more eutectic is present during the latter stages of solidification. Stresses in the solidifying matrix diminish and if flaws occur, they can backfill with excess eutectic. During welding, the amount of eutectic fluid produced at lower solute contents increases, and the maximum crack susceptibility occurs at solute contents below the limit of maximum solid solubility. Under conditions of equilibrium, the amount of eutectic fluid can be estimated by using the lever law, $C_S F_S + C_l F_l = C_O$. The amounts of eutectic under nonequilibrium conditions can be estimated using the Scheil equation, $C_l = C_O F_l^{(k-1)}$. Using these equations we can show that Al 2219, essentially a binary alloy of Al and Cu, would have 2.5% eutectic under equilibrium conditions, but has over 13% terminal eutectic fluid under nonequilibrium conditions. Al 2195, is a true ternary alloy and it is more difficult to estimate the amounts of terminal fluid. However, upper limits for the amount of fluid can be estimated as < 1% in the equilibrium case and , < 6% in the nonequilibrium case.

Al 2219 is essentially saturated with copper rich second phase materials, particularly in the weld region. On a microscopic scale, myriad anode cathode pairs exist and corrosion proceeds at many locations simultaneously. Al 2195, however exhibits regions of pronounced depletion adjacent to solute rich regions. Moreover, the depleted regions are often subject to microfissuring, providing preferred sites for localized corrosion. The transient stresses associated with the welding thermal cycle produce a macroscopic segregation of microconstituents through a "squeezing" mechanism during the welding cycle as described by Walsh and Nunes. This region can be identified on the surface of welds in both Al2219 and Al 2195, which exhibit narrow bands of exuded material in the fusion line region. The fine equiaxed region in Al 2195, an unmixed region, is enriched in terminal transient. The extensive adjacent PMZ is often starved of eutectic liquid, and is subject to hot cracking during the welding process. This location was found to be particularly sensitive to localized attack.

Table 1 provides a summary of the corrosion data gathered during this investigation. Figures 1 and 2 show typical histories for particular samples.

TABLE 1 CORROSION SUMMARY

MATERIAL	CONDITION	MEDIUM	AVERAGE	MAXIMUM	SLOPE
2195	BM	MC BIO	0.965	3.709	0.14
2219	HW	MC	0.535	1.36	0.012
2195	HW	MC	0.476	1.59	0.0195
2195	AW	MC	0.461	1.123	0.0221
2219	AW	MC	0.255	0.439	-0.004
2195	BM	SLT	0.250	0.8583	-0.0158
2195	BM	MC	0.245	0.6943	0.0266
2219	BM	SLT	0.221	0.6335	-0.0068
2219	BM	MC	0.204	0.4059	0.0004
2195A	BM	MC	0.200	0.3651	0.0266

CONCLUSIONS

Results indicate that for base metal samples, corrosion in mild corrosive water was more severe than corrosion in salt water, examination of test samples indicated that a uniform layer of passivating coating formed over the sample during the early stages of exposure and no stable pits developed in either alloy. High initial rates in both Al 2219 and Al 2195 indicates that corrosion was occurring at many locations over the surface, no preferred locations or stabilized pits developed, and a passivating coating formed over the surface. In mild corrosive water however, initial corrosion rates were lower and preferred sites developed. Welding was found to increases the corrosion rate in Al 2195 and Al 2219, creating strong local galvanic couples on the microscopic scale. More importantly, welding causes severe localized pitting in Al 2195 samples. Figure 3 shows severe localized pitting along the PMZ in a Al 2195 weld. Note the fine equiaxed region with the extensive amount of cathodic second phase adjacent to the severely corroded PMZ. Note the attack proceeding into the base material and the textured pancake structure. This localized attack was typical of Al 2195 welds and was not observed in Al 2219. Figure 4 shows the HAZ region in Al 2195. Note the hot cracking and porosity . Autogenously welded Al 2195 samples were more susceptible to attack than heterogeneously welded Al 2195 samples because there were microtears in the partially melted zone of autogenous samples. Autogenously welded Al 2219 samples were less susceptible to corrosion than autogenously welded Al 2195 samples because alloy 2219 is designed to "backfill" any flaws that form with copious amounts of eutectic liquid. Heterogeneously welded samples in both materials had high corrosion rates, but only the Al 2195 material was subject to localization of attack. The partially melted zones of Al 2195 samples were subject to severe, focused attack. In all cases, interdendritic constituents in welded areas and intergranular constituents in base material were cathodic to the al rich matrix materials. Al 2219 samples were subject to crevice corrosion. Biologically active media (an inoculation of 30 cc of KFC water in a 1000cc mild corrosive water test unit) greatly increased the corrosion rate in the single 2195 sample studied. Galvanic studies show both organic and inorganic zinc primers protect grit blasted Al 2219. The inorganic zinc

primer studied was very sensitive to coating procedure. AC Impedance studies show that the pore resistance (r_p) and charge transfer resistance (r_t) of the organic zinc coating increase rapidly with time.

REFERENCES

1) C. J. Peel, The Development of Aluminum-Lithium Alloys: An Overview, Conference Proceedings, Fifth International Aluminum-Lithium Conference.
2) Starke, E.A. Jr. and Quist, William E., The Microstructure and Properties of Aluminum- Lithium Alloys, Conference Proceedings, Fifth International Aluminum-Lithium Conference.
3) Y. A. Chang and S.W. Chen, Microsegregation in Solidification for Ternary Alloys, Met. Trans. A, Volume 23A, march 1992.
4) Y.A. Chang et. al., Calculation of Phase Diagrams and Solidification Paths of Al Rich Al-Li-Cu Alloys, Met. Trans. A, Volume 2A, December 1991.
5) K. Moore et. al., Effect of Copper Content on the Corrosion and Stress Corrosion Behavior of Al-Cu-Li Weldalite Alloys, Aluminum-Lithium Alloys, Vol III
6) R.G. Buchheit, F.D. Wall and J.P. Moran, An Anodic Dissolution Based Mechanism for the rapid cracking Pre-Exposure Phenomenon Demonstrated by Al-Li-Cu Alloys, NACE, Corrosion 94, Baltimore, MS. Paper #623.
7) M. Stern, Theoretical Basis of the Polarization Resistance Technique, Corrosion, Vol. 14, 1958, p 410t.
8) D. S. Gnanamuthu, R.J. Moore, LASER Welding of 8090 Al-Li Alloy, Proceedings of International Power Beam Conference, San Diego, CA May 2-4, 1988.
9) T.A. Marsico, R. Kossowski, Physical properties of Laser Welded Al alloy 2090. Conference Proceedings, Fifth International Aluminum-Lithium Conference, Williamsburg Va., March, 1989.
10) P. Bourgwasser, et. al., Intergranular Fracture of Al-Li-Cu-Mg Alloy Resulting from Non-equilibrium Eutectic Melting During Solution Treatment. Materials Science and Technology, Vol 5, 1989.

Figure 1

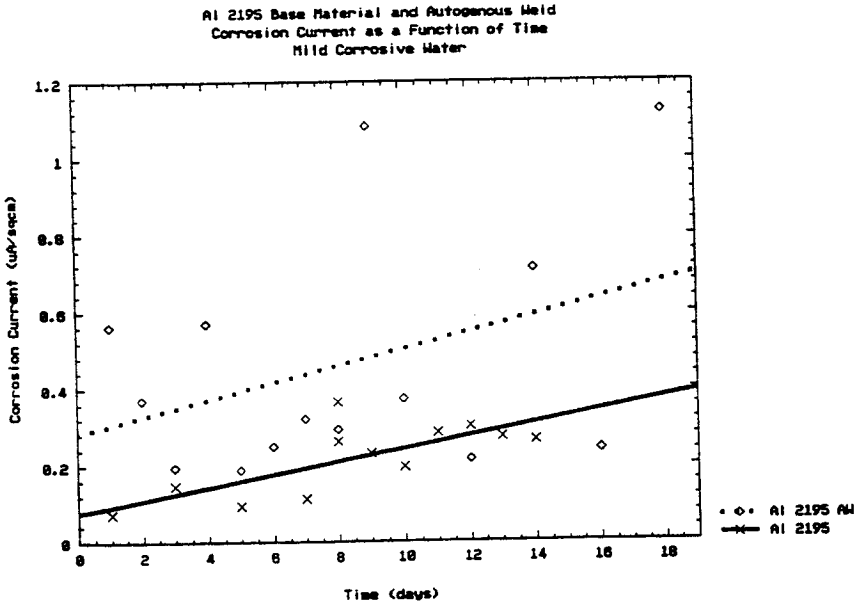

Figure 2

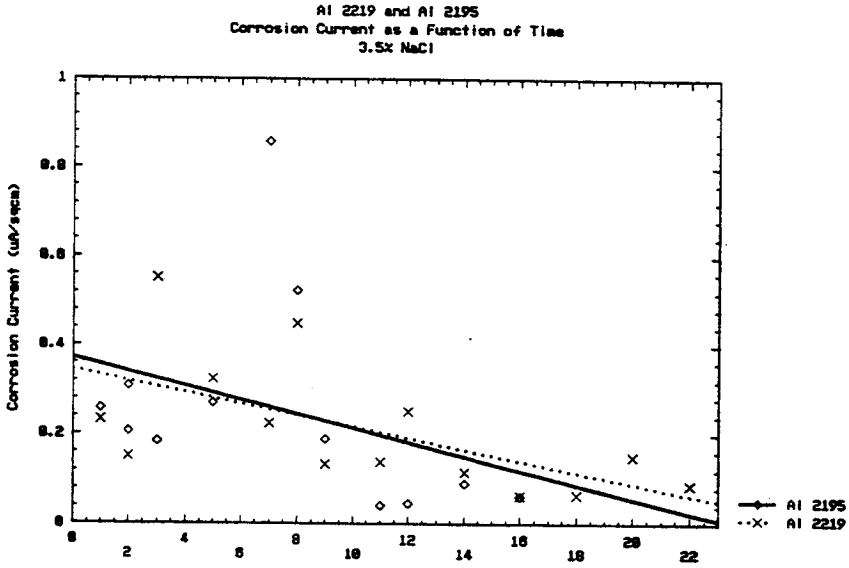

Figure 3. Localized PMZ Attack

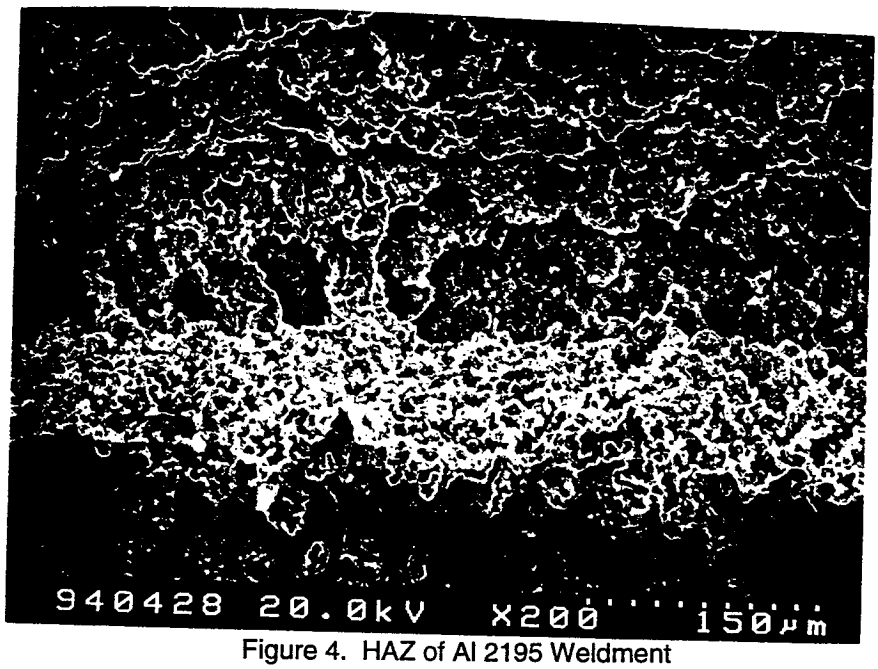

Figure 4. HAZ of Al 2195 Weldment